The Effects of Physiological and Methodological Determinants on ^{18}F-FDG Mouse Brain Imaging Exemplified in a Double Transgenic Alzheimer Model

Steven Deleye, MSc[1], Ann-Marie Waldron, MSc[1], Jill C. Richardson, PhD[2], Mark Schmidt, PhD[3], Xavier Langlois, PhD[3], Sigrid Stroobants, MD, PhD[1,4], and Steven Staelens, PhD[1]

Abstract

Introduction: In this study, the influence of physiological determinants on 18F-fluoro-D-glucose (^{18}F-FDG) brain uptake was evaluated in a mouse model of Alzheimer disease.

Materials and Methods: TASTPM (Tg) and age-matched C57BL/6 J (WT) mice were fasted for 10 hours, while another group was fasted for 20 hours to evaluate the effect of fasting duration. The effect of repeatedly scanning was evaluated by scanning Tg and WT mice at days 1, 4, and 7. Brain ^{18}F-FDG uptake was evaluated in the thalamus being the most indicative region. Finally, the cerebellum was tested as a reference region for the relative standard uptake value (rSUV).

Results: When correcting the brain uptake for glucose, the effect of different fasting durations was attenuated and the anticipated hypometabolism in Tg mice was demonstrated. Also, with repeated scanning, the brain uptake values within a group and the hypometabolism of the Tg mice only remained stable over time when glucose correction was applied. Finally, hypometabolism was also observed in the cerebellum, yielding artificially higher rSUV values for Tg mice.

Conclusion: Corrections for blood glucose levels have to be applied when semiquantifying ^{18}F-FDG brain uptake in mouse models for AD. Potential reference regions for normalization should be thoroughly investigated to ensure that they are not pathologically affected also by afferent connections.

Introduction

Positron emission tomography (PET) is a noninvasive imaging technique that permits in vivo monitoring of physiological and pathological processes.[1] A common PET radiotracer frequently employed in clinical and preclinical studies is 2-deoxy-2-^{18}F-fluoro-D-glucose or ^{18}F-FDG.[2-4] As a glucose analogue, ^{18}F-FDG is used to assess glucose metabolism and is mainly employed for tumor and brain imaging, as these tissues have a large metabolic demand. In Alzheimer Disease (AD), ^{18}F-FDG has been long validated as a neuroimaging biomarker and is used as a surrogate measure of synaptic activity.[5] The ^{18}F-FDG is useful both for diagnosis and for disease monitoring in AD. Decreases in ^{18}F-FDG uptake correlate with cognitive impairment along the continuum from normal cognitive status over mild cognitive impairment (MCI) to AD dementia.[6] The

reductions in ^{18}F-FDG uptake indicate a reduction in neuronal energy demand, mainly arising from synaptic dysfunction and loss caused by β-amyloid and tau pathology. Also, losses of

[1] Molecular Imaging Center Antwerp, University of Antwerp, Antwerp, Belgium
[2] R&D China UK Group, GlaxoSmithKline, Stevenage, United Kingdom
[3] Neuroscience Department, Janssen Pharmaceutica NV, Beerse, Belgium
[4] Nuclear Medicine Department, University Hospital Antwerp, Antwerp, Belgium

Corresponding Author:
Steven Staelens, Department of Nuclear Medicine, Faculty of Medicine and Health Sciences, Molecular Imaging Center Antwerp, University of Antwerp, Universiteitsplein 1, 2610 Antwerp, Belgium.
Email: Steven.Staelens@uantwerpen.be

neurons and neuropil containing neurofibrillary tangles[7] contribute to the reduction in glucose consumption.[5,8] Advances in small animal PET (μPET) have made imaging possible in mouse models of AD,[9,10] allowing longitudinal follow-up[11,12] and thus facilitating translation of knowledge from bench to bedside. The utility of ^{18}F-FDG as a preclinical biomarker for investigation of AD processes in animal models has been debatable, as states of hyper-,[13,14] normo-,[15,16] and hypometabolism[17] have been described in transgenic mouse models. The reported inconsistencies could reflect true biological differences between transgenic models, as these differ in their pathological severity due to the type and number of mutations they possess and the age of the animals. Alternatively, the inconsistencies could be due to methodological differences between studies with conflicting reports of ^{18}F-FDG uptake within the same transgenic strains, Tg2576[13,15] and 5xFAD,[9,18] supporting this hypothesis. The biodistribution of ^{18}F-FDG and its uptake into target tissues is influenced by a wide variety of physiological, pharmacological, and methodological factors.[19,20] Hence, it is possible that the reported differences between the transgenic mouse models are in actuality artifacts due to methodological inconsistencies and are not representative of inherent pathological processes.

It is therefore important that these ^{18}F-FDG imaging protocols are standardized eliminating confounding factors, as these can potentially alter the outcome of the experiment. Most ^{18}F-FDG imaging studies, including those in imaging for AD, make use of semiquantitative measures: the percentage of injected dose (%ID/g) or the standard uptake value (SUV), thereby eliminating the need for long scan durations or invasive catheterization to obtain the plasma input function required for absolute quantification. The %ID/g represents the ratio of tissue uptake and the injected dose, while SUV additionally normalizes the %ID/g by the body weight of each individual animal. Without a standardized protocol, these measures can be biased by confounding factors both in humans[21,22] and in small animals.[23] There have been several comprehensive studies investigating potential influencing factors such as blood glucose levels,[20,24,25] the administration route,[20] fasting,[20,23,24] anesthesia,[23,26-29] body temperature,[23] and stress.[24,30-32] Most of these influence ^{18}F-FDG uptake by directly changing the blood glucose levels or by altering the glucose need. The glucose need, and thus the ^{18}F-FDG uptake, will be lower with higher endogenous glucose levels. Stress (ie, corticosterone) and anesthesia such as isoflurane and ketamine cause endogenous glucose levels to increase. Fasting on the other hand lowers endogenous glucose levels. A low body temperature will cause a higher glucose need and thus higher ^{18}F-FDG uptake in the brown fat tissue.

In this study, we use double transgenic TASTPM mice[33] as our experimental model of cerebral amyloidosis, as these mice have been reported to demonstrate cerebral hypometabolism with increasing age by both ex vivo[34] and in vivo measurements.[35,36] We aim to quantify the possible confounding effects of fasting duration, repeatedly scanning, and a normalization method on the differential ^{18}F-FDG brain uptake in these TASTPM (transgenic, Tg) mice versus wild-type (WT) littermate controls. In particular, we search for the best approach to normalize for physiological determinants such as glucose and body weight.

Materials and Methods

Animals

TASTPM mice overexpress the hAPP695swe mutation and the presenilin-1 M146 V mutation under the control of the neuron-specific Thy-1 promoter. These mice display accelerated amyloid deposition with plaques forming as early as 3 months. The cerebral Aβ 1-42 load is greater and results in the formation of dense core amyloid plaques.[37] Age-matched C57BL/6 J littermates were used as controls (WT). Mice (n = 25 Tg; n = 26 WT, male) were 14.29 ± 0.76 (standard deviation) months of age and were treated in accordance with the European Ethics Committee (decree 86/609/CEE). The study protocol was approved by the local Animal Experimental Ethical Committee of the University of Antwerp, Belgium (2012-25). The animals were kept under environmentally controlled conditions (12-hour light–dark cycle, 20°C-24°C and 40%-70% relative humidity) in individually ventilated cages with food (ssniff R/M-H; Bio Services, the Netherlands) and water ad libitum. The animals were housed in type M3 cages with 1 male animal per cage and received environmental enrichment. TASTPM animals and their littermate controls were received in kind from GlaxoSmithKline (Stevanage, United Kingdom) through the PharmaCog consortium.

Radiosynthesis of ^{18}F-FDG

The ^{18}F-FDG was synthesized using a cassette-based GE Fastlab synthesis module (GE Healthcare, Belgium). ^{18}F-fluoride was produced by bombarding ^{18}O-enriched water using a 11-MeV proton beam in an Eclips HP cyclotron (Siemens, Knoxville, Tennessee). The purified ^{18}F-FDG was then diluted with 0.9% NaCl (Baxter, Belgium) and sterile filtered through a 0.22 μmol/L filter. Quality control was performed according to European Pharmacopoeia 7.1. Radiochemical identity was confirmed by high-performance liquid chromatography (HPLC; Dionex; ThermoFisher, Belgium) and radio thin-layer chromatography. Radiochemical purity was determined by HPLC (Dionex, ThermoFisher, Belgium) and ranged from a minimum of 99.56% to a maximum of 99.97%. Radionuclidic identity and purity were confirmed by gamma spectrum analysis (Multi-channel analyzer, Canberra).

Image Acquisition and Processing Protocols

Based on the protocol previously used in TASTPM mice,[35] the animals were injected awake with an intravenous tail vein injection of 18.5 MBq of ^{18}F-FDG in a solution of 0.2 mL. Static μPET scans of 20 minutes were acquired after a conscious uptake period of 45 minutes. Anesthesia was induced by inhalation of isoflurane (5% for induction and 2% for maintenance during preparation and scanning) supplemented with

oxygen. Respiration rate and body temperature of the animal were constantly monitored (BioVet, USA) during the entire scanning period. The core body temperature of the animals was maintained via a temperature controlled heating pad.

The PET imaging was performed using 2 Siemens Inveon PET-CT scanners (Siemens Preclinical Solution, Knoxville, Tennessee).[38] The scanner utilizes $1.59 \times 1.59 \times 10$ mm lutetium oxy-orthosilicate crystals grouped in 20×20 blocks. The axial and transaxial field of views are 127 and 100 mm, respectively. The animals were scanned in a feet-first-prone position. The energy and timing window were set to 350 to 650 keV and 3.432 nseconds, respectively. The PET images were reconstructed using 4 iterations with 16 subsets of the 2-dimensional ordered subset expectation maximization (OSEM 2D)[39] algorithm following Fourier rebinning (FORE).[40] Normalization, dead time, random, CT-based attenuation and single-scatter simulation (SSS) scatter corrections[41] are applied. The PET images are reconstructed on a $128 \times 128 \times 159$ grid with a pixel size of 0.776 mm and a slice thickness of 0.796 mm. The CT imaging was done using a $220°$ rotation with 120 rotation steps. Voltage and amperage are set to 80 keV and 500 µA, respectively. The CT images were reconstructed using the Feldkamp filtered-backprojection algorithm.

Each individual PET image was transformed into the space of a standard FDG PET template[42] using brain normalization in PMOD v3.3 (PMOD Technologies, Switzerland). These spatially normalized images were then analyzed using an magnetic resonance imaging mouse whole brain volume-of-interest (VOI) template[43] available in the same software package and a priori coregistered with the FDG PET template. As the scanner was calibrated using a uniform cylinder of activity, whole brain VOI statistics in kBq/cm^3 are generated and used to calculate different quantification methods: the percentage of injected dose per gram ($\%ID/g = 100 \times$ radioactivity concentration in VOI/injected radioactivity) and the SUV ($=\%ID/g \times$ body weight) without and with ($\%ID/g_{glc} = \%ID/g \times glc$ and $SUV_{glc} = SUV \times glc$) correction for the blood glucose level.

Study Design

In order to design a robust and reproducible imaging protocol, we investigated the effect of fasting duration and of repeatedly scanning as physiological determinants for quantification. Also, we evaluated relative SUV (rSUV) as a methodological determinant for normalization of regional uptake values to a reference region.

The effects of prolonged fasting. TASTPM (n = 13) and age-matched (15 ± 0.02 months) littermate WT mice (n = 14) were divided into 2 groups of different fasting duration. One group (WT n = 7, Tg n = 6) was fasted for 10.41 ± 0.35 (standard error of the mean, SEM) hours and the other group (WT n = 7, Tg n = 7) for 19.77 ± 0.01 (SEM) hours. Baseline and prescan whole blood glucose (mg/dL) were measured (in duplo; One Touch Ultra 2, Lifescan, France) as well as body weight. As the thalamus has been previously shown to
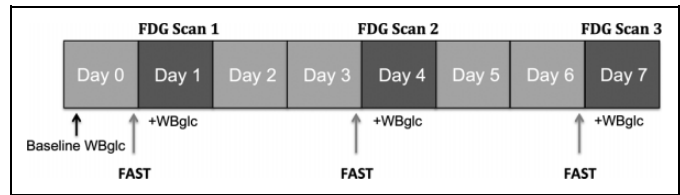

Figure 1. Experimental design to investigate the confounding effects of repeatedly scanning on 18F-fluoro-D-glucose (^{18}F-FDG) uptake.

demonstrate the most significant decreases in glucose utilization,[34,35] we selected it as a representative hypometabolic region for our investigations.

The effects of repeatedly scanning. A subset of mice, TASTPM (n = 6) and age-matched littermates (n = 7; 15 ± 0.02 months), used in the prolonged fasting experiment (the 10 h fasting group) was scanned 3 consecutive times at day 1, 4, and 7 resulting in an interscan duration of 2 days (Figure 1). Baseline and prescan whole blood glucose was measured and ^{18}F-FDG uptake was evaluated in the thalamus as described earlier.

The effects of a reference region. TASTPM (n = 12) and age-matched (13.5 ± 0.02 months) littermates WT (n = 12) mice were scanned with ^{18}F-FDG after fasting for 10.45 ± 0.25 (SEM) hours. Prescan whole blood glucose and body weight were measured. Here, the rSUV was additionally calculated as a normalization method in addition to the employed quantification measures in the previous experiments (The effects of prolonged fasting and The effects of repeatedly scanning sections). The cerebellum was chosen as the reference region, as it is generally devoid of amyloid plaques. Brain ^{18}F-FDG uptake was evaluated in the striatum, cortex, hippocampus, thalamus, cerebellum, basal forebrain and septum, hypothalamus, amygdala, brain stem, cingulate cortex, superior colliculi, midbrain, and inferior colliculi.

Statistical Analysis

Data were analyzed using SPSS v23 and GraphPad Prism 6.0b (GraphPad Software Inc, San Diego, California) and presented as mean $\pm$ SEM. After verifying the normality and the homoscedasticity of the data using, respectively, the Shapiro-Wilk test and the Levene test, parameteric tests were used. A Student (2-tailed, unpaired) t test was performed to compare the tracer uptake between Tg and WT animals. Repeated measure analysis of variance was performed to test the glucose level differences over time in the effects of repeatedly scanning experiment.

Results

Glucose Correction is Mandatory if Duration of Fasting Varies

Baseline glucose levels are lower for the Tg mice than for WT as shown in Figure 2A as an inherent genotype effect
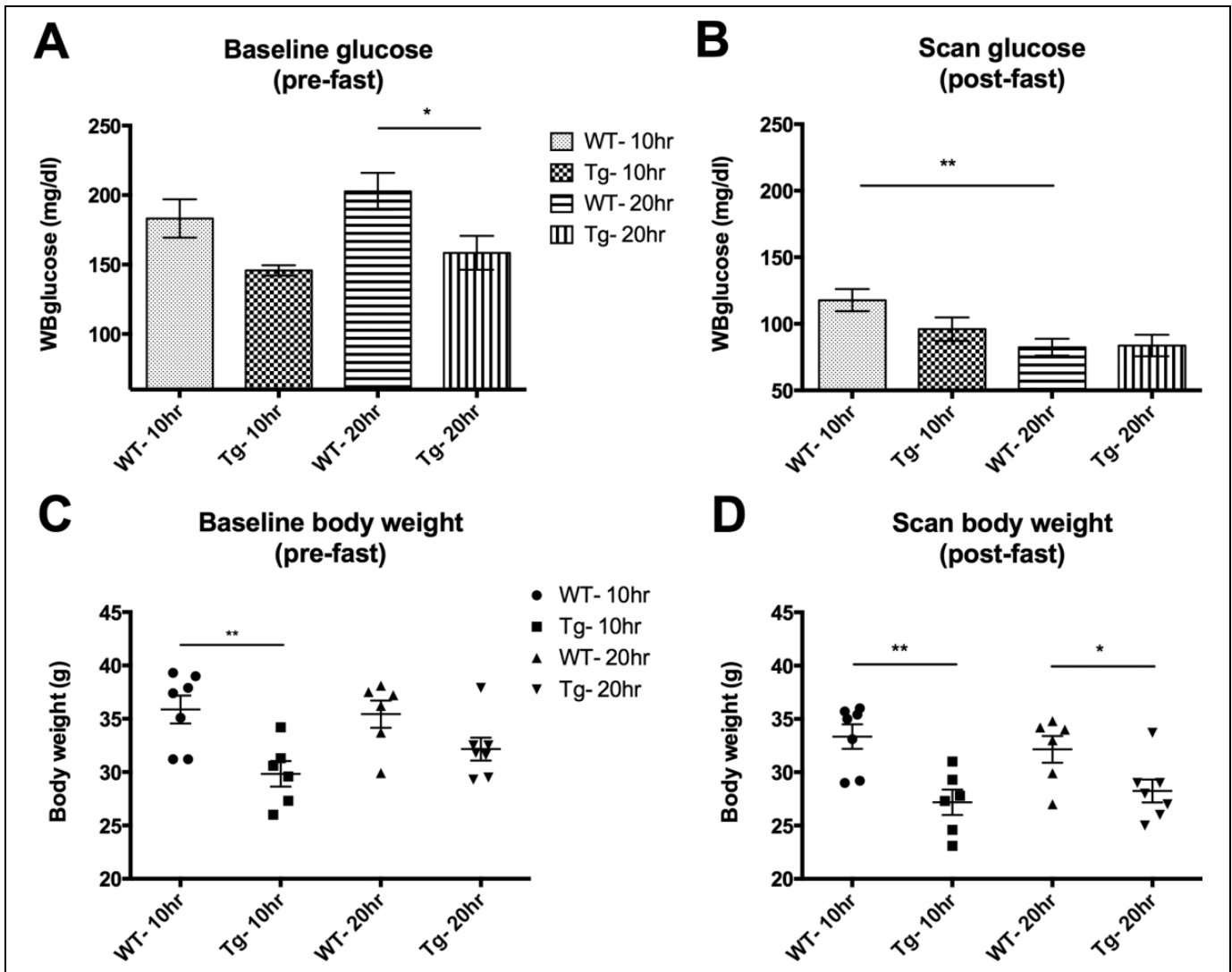
Figure 2. Whole blood glucose levels and body weights measured at the baseline (A and C respectively) and before the scan (B and D respectively) of the WT and Tg mice for the different fasting durations (*P < .05; **P < .01).

(significant depending on group allocations). Both fasting durations (10.41 ± 0.35 and 19.77 ± 0.01 hours, respectively) induced substantial reductions in scan blood glucose after fasting as shown in Figure 2B. For those animals that were fasted only for 10.41 ± 0.35 hours, the differences between Tg and WT persisted with transgenic animals still exhibiting lower blood glucose levels albeit not significant. Blood glucose levels were comparable between genotypes for those animals that were fasted longer. Figure 2C shows that also the baseline body weights are lower for the Tg mice than for WT as an inherent genotype effect (significant depending on group allocations). Figure 2D demonstrates that this lower body weight for the Tg compared to WT remains after fasting for both fasting durations. The loss in body weights of all mice decreased after fasting within a range of minimum 5.70% and maximum 14.68% body weight.

Without a correction for varying blood glucose levels as for %ID/g and SUV, a significantly higher uptake in the 20-hour fasting group is measured not necessarily representing an intrinsically higher cerebral metabolism but rather due to less competing endogenous glucose as exemplified in Figure 3 for the thalamus. This artificial difference in uptake was adequately attenuated with glucose correction as demonstrated for %ID/g$_{glc}$ and SUV$_{glc}$. Further, Figure 3 also shows that for these latter 2 glucose-corrected measures, a trend toward the anticipated hypometabolism[35,36] is demonstrated for both fasting durations and is significant for the Tg animals in the 20-hour group if measured with SUV$_{glc}$. Noteworthy is that SUV$_{glc}$ is known to be a linear overcorrection for nonlinear ^{18}F-FDG brain uptake[44] when body weight differs significantly (Figure 2D). Importantly, if not correcting for body weight and blood glucose (using %ID/g), the reported hypometabolism[35,36] can be misinterpreted as hypermetabolism for the group of animals fasted for 10 hours, as these are displaying a trend toward higher uptake for the thalamus. Figure 4 strikingly illustrates the impact of the physiological determinants on
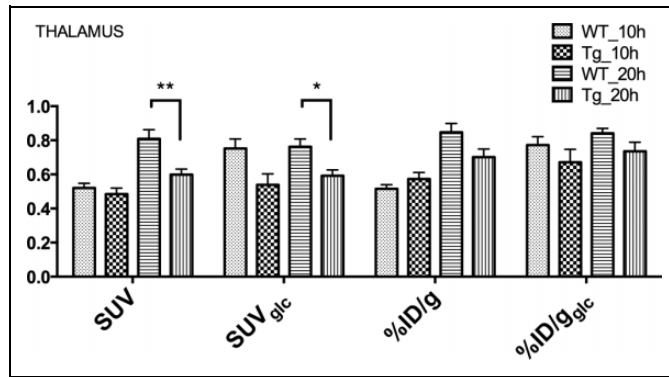
Figure 3. Overview of the different quantification methods in the WT and Tg mice for the 10 hours and 20 hours fasting durations. Uptake is measured in the thalamus (THA; *P* < .05; **P* < .01). Significance between 10- and 20 hours of fasting is not plotted for clarity.

the average group images with SUV_{glc} and $\%ID/g_{glc}$ demonstrating the lowest variability if fasting durations varies for both WT and Tg animals, and SUV_{glc} and $\%ID/g_{glc}$ also confirming the expected hypometabolism of Tg versus WT animals,[35,36] for both fasting durations with a linear overcorrection for SUV_{glc} (see Figure 2D).

Glucose Correction Accounts for the Effect of Repeated Scanning

In comparison to the baseline whole blood glucose levels, initial exposure to fasting for the first scan session (scan 1) induced a substantial decrease in blood glucose levels for both genotypes (Tg; *P* < .05) as anticipated. However, upon repeated exposure to fasting for scan 2 and 3, these reductions in blood glucose become largely attenuated, with the blood glucose
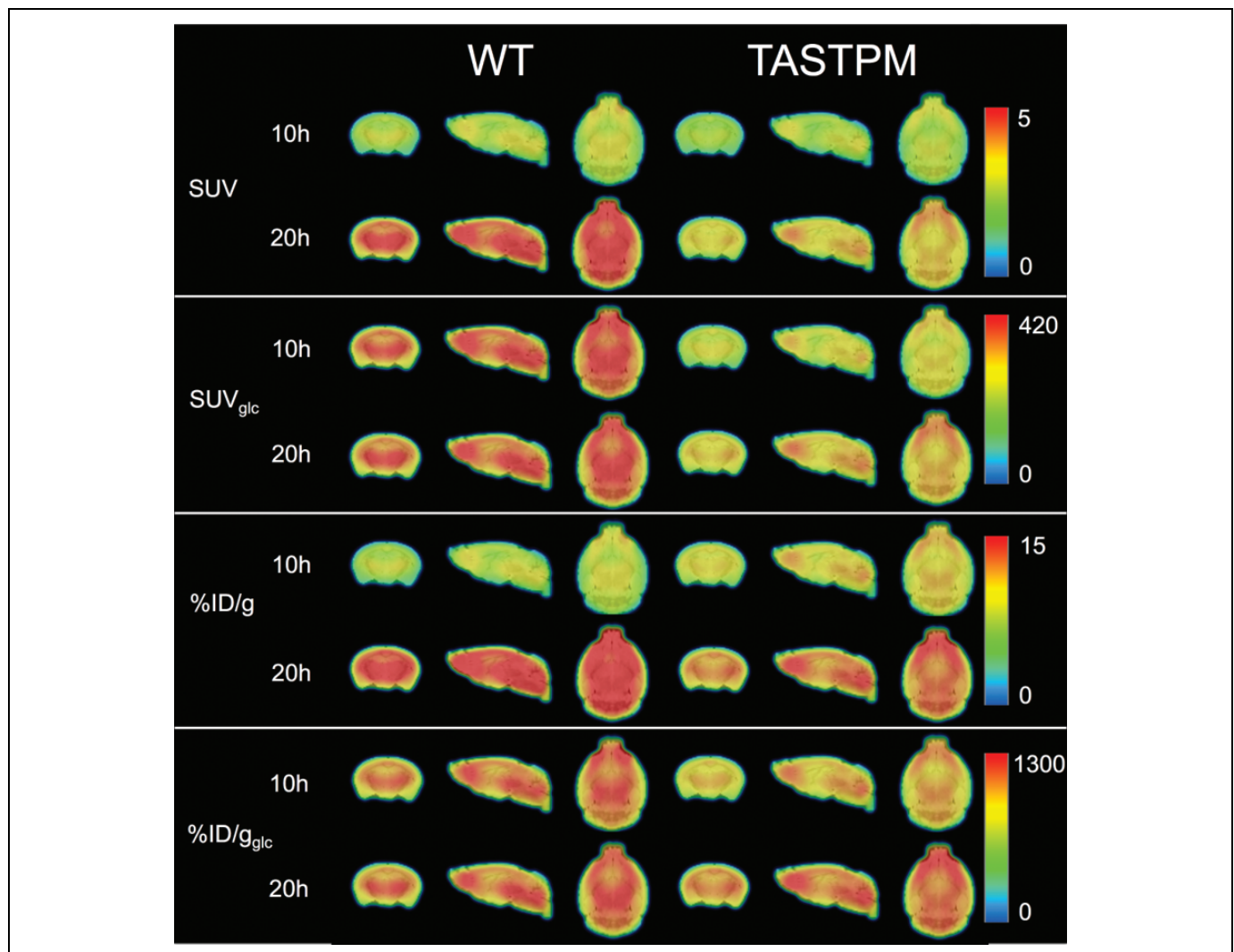

Figure 4. Semiquantitative measures standard uptake value (SUV), SUVglc, percent injected dose (%ID/g), $\%ID/g_{glc}$ expressed as average brain images of the WT and Tg mice for the 10- and 20-hour fasting durations.
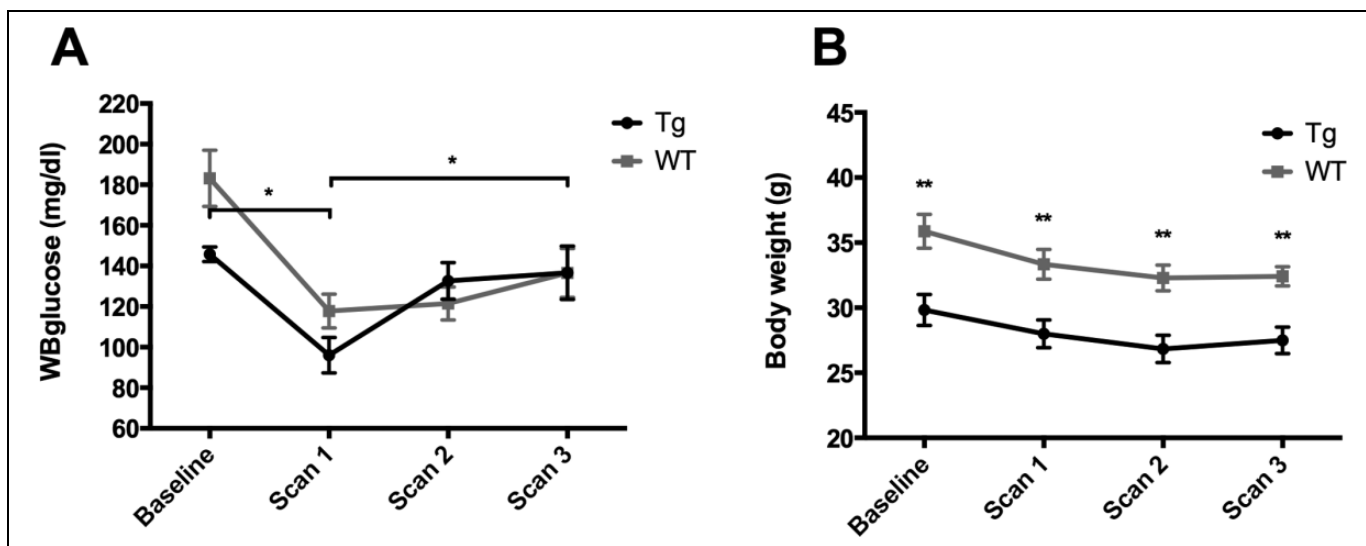
Figure 5. Glucose (A) and body weight (B) changes over time of the WT and the Tg mice (*$P < .05$, **$P < .01$).

levels of Tg mice for the third scan session (scan 3) essentially even reaching the baseline glucose levels as demonstrated in Figure 5A.

An initial exposure to fasting for the first scan caused also a nonsignificant decrease in body weight for both genotypes followed by a more stable evolution for later scans (Figure 5B). The loss in body weights of all mice in percentage of the baseline body weight was within a range of minimum 6.07% and maximum 14.04%.

Overall, Figure 6 shows that the brain uptake values within group remained more stable over time with various scan sessions only when glucose correction was applied (%ID/g$_{glc}$ and SUV$_{glc}$). When additionally correcting for animal weight (SUV$_{glc}$), the anticipated hypometabolism[35,36] for Tg animals is significant in the thalamus at scans 1 and 2. However, caution is warranted as a linear correction for body weight might overestimate differences between groups with nonnegligible body weight differences. Noteworthy, if not correcting for glucose levels and body weight (%ID/g), an erroneous hypermetabolism may be concluded for the Tg mice after the first scan session, again illustrating the critical importance of correcting for these physiological determinants. This is also demonstrated in Figure 7, as group-averaged images only remain stable over scan sessions and consistently show hypometabolism of Tg versus WT if corrected for whole blood glucose levels. Additionally, a linear correction for body weight might overestimate the intergroup differences in brain glucose metabolism (see Figure 5B).

The Cerebellum is not an Appropriate Reference Region in TASTPM Mice

The body weights of the WT mice (31 g $\pm$ 1.2) were significantly ($P < .05$) higher than the Tg mice (28 $\pm$ 0.6 g), and there was no significant difference between the glucose levels of the
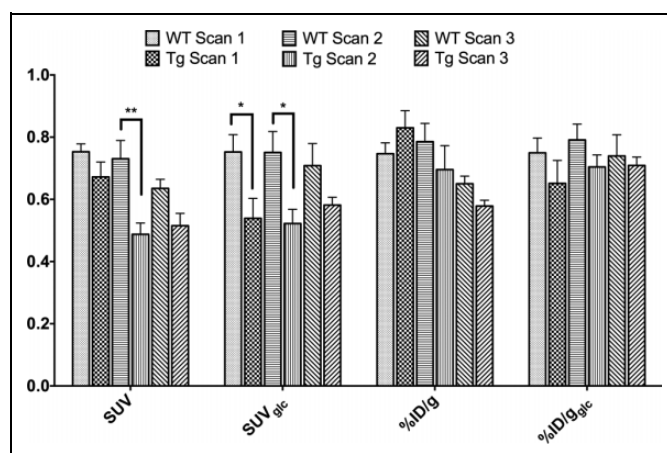

Figure 6. Graph representing the different image quantifications percent injected dose (%ID/g) and standard uptake value (SUV) with and without glucose correction for the thalamus in WT and Tg mice on the different scan days.

Tg (128.7 $\pm$ 9.6) and the WT (128.1 $\pm$ 5.2 mg/dL) mice after 10.45 $\pm$ 0.25 hours of fasting.

Figure 8 shows that when correcting for blood glucose levels (%ID/g$_{glc}$, SUV$_{glc}$) a significant hypometabolism is measured as expected[35,36] and is the largest for SUV$_{glc}$ potentially being an overestimation due to linear overcorrecting for significant intergroup body weight differences. When not correcting for body weight or glucose (%ID/g), this significant hypometabolism is lost. Importantly, all quantification methods demonstrate that also the cerebellum has a lower brain uptake (SUV and SUV$_{glc}$; $P < .05$) of ^{18}F-FDG. Hence, normalizing to the cerebellum (rSUV) as a reference region yielded higher values for Tg (Figure 8), thereby largely eliminating the observed hypometabolism as evaluated with the other quantification measures and even resulting in a trend toward hypermetabolism for some regions.
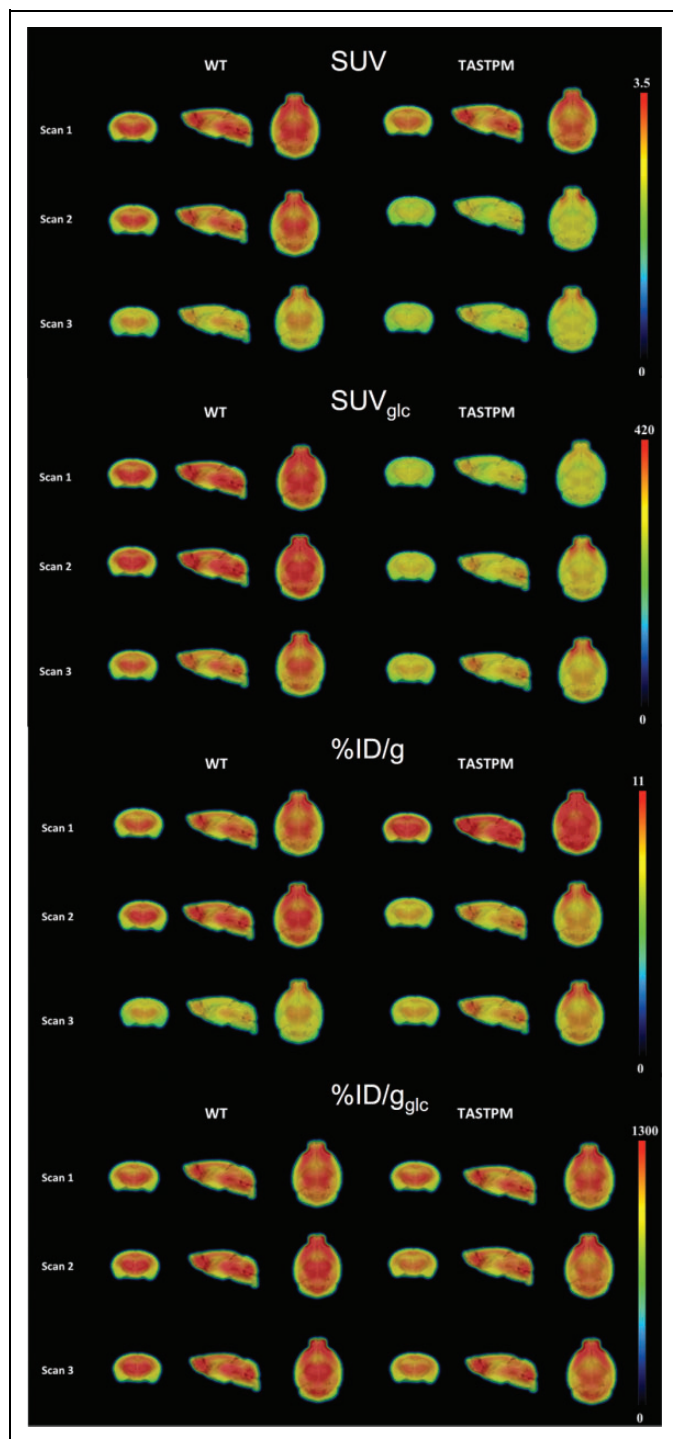
Figure 7. Standard uptake value (SUV), SUV$_{glc}$, percent injected dose (%ID/g), and %ID/g$_{glc}$ average images showing the different 18F-fluoro-D-glucose (^{18}F-FDG) brain uptake between WT and Tg mice.

Discussion

Clinical ^{18}F-FDG PET studies of patients with AD show a decreased cerebral metabolism both in brain regions affected by Aβ plaque deposition as well as in pathology-free regions.[8,45] It has been shown that these regions affected by Aβ match those brain areas with increased ^{18}F-FDDNP and

^{11}C-PiB retention.[46,47] In the preclinical field, a lot of conflicting data are reported whether transgenic models demonstrate hyper-,[13,14] hypo-,[17] or normometabolism,[15,48] with ^{18}F-FDG PET in comparison to healthy controls. Nevertheless, ^{18}F-FDG as a preclinical biomarker would improve the predictability of drug discovery and development efforts by improving the congruency of preclinical models to clinical reality. Therefore, there is a need to investigate the physiological and methodological factors that can possibly confound the results in such preclinical AD research studies.

Fueger et al[23] already demonstrated the need to fasten (8-12 hours) animals before a ^{18}F-FDG PET scan in order to lower plasma glucose levels and to reduce ^{18}F-FDG uptake in skeletal muscle and brown fat to achieve a higher brain uptake. In our study, we showed that even a higher brain uptake was observed when fasting duration was 19.77 ± 0.01 hours in comparison to 10.41 ± 0.35 hours mainly due to decreasingly low blood glucose levels and not necessarily reflecting altered cerebral glucose metabolic rate. Therefore, it is advisable to always correct for blood glucose levels in order to attenuate any differences in ^{18}F-FDG brain uptake due to different fasting durations. Noteworthy is that when fasting, the mice for 10.41 ± 0.35 hours the inherent difference in plasma glucose levels between WT and Tg mice was maintained, while 19.77 ± 0.01 hours of fasting completely attenuated this difference. Such can be due to increased serum corticosterone levels as Tg mice could be more sensitive to fasting stress by food deprivation, as we and others have previously shown for rats when fasted for 24 hours[24,49] as well as by scan manipulations. However, when animals need to be repeatedly scanned within a short period of time, prolonged fasting leads to substantial weight loss, and fasting durations are preferably much shorter than 19.77 ± 0.01 (8-12 hours). Indeed, Jensen et al[50] summarized the effects of fasting of mice such as changes in hormone balance, body weight, and metabolism among other effects and showed that these changes become larger with longer (overnight) fasting times, as mice consume two-thirds of their total food intake during the night and have a higher metabolic rate than humans. In our study, fasting was done by removing the food pellets and changing the bedding material. This however does not prevent the mice from eating the bedding material and newly produced feces. For this reason, placing the mice on a grid floor during fasting has been recommended[50] but has its implications on animal welfare.

In such a setting with repeatedly scanning and short interscan durations, one equally has to take the blood glucose into account when quantifying the ^{18}F-FDG brain uptake as levels rise over time with the scan sessions (and even more so in Tg mice) for the same reasons. We show here that with repeated scanning, glucose corrected uptake values did not only remove the glucose-induced variability in ^{18}F-FDG uptake over time with scan sessions but also demonstrated the difference between WT and Tg mice more significantly.

In our study, the measures accounting for body weight (SUV and the SUV$_{glc}$) revealed larger differences between WT and Tg mice compared to the other (%ID/g and %ID/g$_{glc}$) metrics,
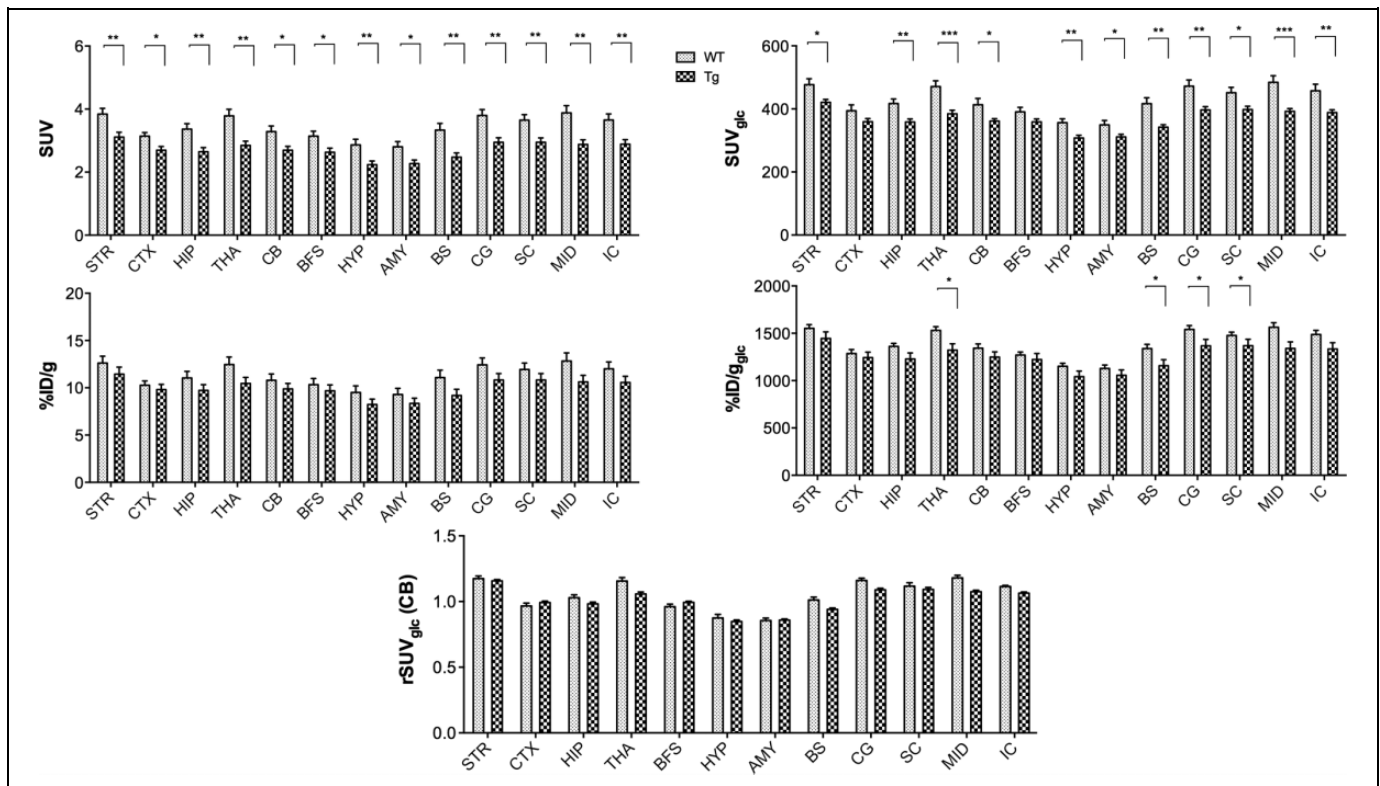
Figure 8. Graphs representing the different quantification measures percent injected dose (%ID/g) and standard uptake value (SUV) with and without glucose correction and also the relative SUV for WT and TG mice. Uptake is measured in the striatum (STR), cortex (CTX), hippocampus (HIP), thalamus (THA), cerebellum (CB), basal forebrain and septum (BFS), hypothalamus (HYP), amygdala (AMY), brain stem (BS), cingulate cortex (CG), superior colliluli (SC), midbrain (MID), and inferior colliculi (IC). *P < .05; **P < .01; ***P < .001.

since SUV_{glc} corrects for the larger volume as WT mice had significantly higher body weights than Tg mice. These SUV measures may however overestimate the actual ^{18}F-FDG uptake if the larger body weight is mostly due to a higher percentage of body fat, as this accumulates relatively little ^{18}F-FDG. Such an overestimation is known in humans[51] and recently also in rodents.[24] Therefore, the use of a lean body weight[51] or a body surface area[52] has been proposed in clinic. As these corrections are however infrequently done, Thie et al[53] proposed a weight sensitivity index for the SUV.

Also, the transgene status of the TASTPM mice could result in a global change in the glucose metabolic rate in the entire mouse or in organs other than the brain. Therefore, the ^{18}F-FDG uptake in the muscle, liver, brown fat, and myocardium was also evaluated (Supplementary Figure S1). A significant difference in muscle uptake was observed between WT and Tg mice for all quantification measures. However, the difference in muscle uptake is very likely more a consequence of reduced (overall) activity of Tg rather than a globally reduced regional metabolic rate of glucose in Tg mice, as these differences are not consistently observed in the other organs.

To avoid all the aforementioned issues related to glucose and body weight, and also with attenuation or calibration, normalization to a reference region is commonly performed. Moreover, such normalization increases statistical power by reducing variability in global flow or metabolism.[17] However,

this approach may yield very inaccurate results if such a reference region is compromised by disease and can thus be a confounding methodological factor. Due to its relative lack of amyloid pathology, the cerebellum is often designated as a reference region.[9,14,54] However, despite the lack of amyloid deposits, we demonstrated a lower ^{18}F-FDG uptake in the cerebellum of Tg mice compared to WT with all quantification measures used which might be caused by amyloid pathology in afferent regions. Waldron et al[35] already showed that regions of decreased ^{18}F-FDG uptake demonstrated by imaging and regions of high amyloid load demonstrated by histology in 13.5 M TASTPM mice are not necessarily correlated.

Applying an rSUV hence leads to comparable ^{18}F-FDG brain uptake in the target regions of Tg and WT, while hypometabolism has been previously proven[35,36] and was confirmed here by us with %ID/g$_{glc}$ and SUV$_{glc}$, which confirms other pathological alternations between Tg and WT mice, besides plaque load in the cerebellum. It is however possible that SUV is not always sensitive enough to pick up early differences between Tg and WT. Macdonald et al,[18] for example, could not distinguish young 5XFAD mice from WT mice until the age of 13 months. In that study, Tg mice could however already be separated from WT at the age of 2 months when comparing the ratios of alternating regions in the same brain.

Besides the aforementioned physiological (glucose, body weight) and methodological (reference region) determinants,

also technical limitations such as spatial resolution have an impact. In mice, regions with high uptake in the head such as the masseter muscles of the jaw or facial glands (salivary, lacrimal, and harderian) may contaminate nearby brain regions due to spillover. On the other hand, the uptake of ^{18}F-FDG in small brain regions may be underestimated due to partial volume effect. The smallest volumes studied here were 8.71 and 7.38 mm³, respectively, from the superior and inferior colliculi, while the other regions were larger than 10 mm³.[43] A study by Welch et al[17] showed that statistical parametric mapping was generally more sensitive than regional analyses, as small clusters of voxels within a VOI can differ significantly even in the absence of significant changes over the whole region. Alternatively, larger rodent species such as transgenic rats expressing mutations related to familial AD have also been proposed[55] and tested.[56]

Conclusion

Corrections for blood glucose levels have to be applied when semiquantifying ^{18}F-FDG brain uptake in mouse models for AD to attenuate the effects of varying fasting durations and the impact of repeatedly scanning. The use of SUV_{glc} is advised over the $\%ID/g_{glc}$, as this measure demonstrates the anticipated ^{18}F-FDG uptake difference between WT and Tg mice more clearly. However, SUV should be carefully considered if significant intergroup (between models) or interscan (longitudinally over time) body weight differences exist. Potential reference regions for normalization should be thoroughly investigated to ensure that they are not pathologically affected also by afferent connections.

Supplemental Material

The online [appendices/data supplements/etc] are available at http://mix.sagepub.com/supplemental

References

1. Alexander GE, Chen K, Pietrini P, Rapoport SI, Reiman EM. Longitudinal PET evaluation of cerebral metabolic decline in dementia: a potential outcome measure in Alzheimer's disease treatment studies. *Am J Psychiatry*. 2002;159(5):738-745.
2. Xi W, Su D, Nie B, et al. 18F-FDG PET study reveals brain functional changes during attention in rats. *J Nucl Med*. 2013; 54(11):1969-1973.
3. Gray KR, Wolz R, Heckemann RA, et al. Multi-region analysis of longitudinal FDG-PET for the classification of Alzheimer's disease. *Neuroimage*. 2012;60(1):221-229.
4. Heylen M, Deleye S, De Man JG, et al. Colonoscopy and µPET/CT are valid techniques to monitor inflammation in the adoptive transfer colitis model in mice. *Inflamm Bowel Dis*. 2013;19(5): 967-976.
5. Attwell D, Laughlin SB. An energy budget for signaling in the grey matter of the brain. *J Cereb Blood Flow Metab*. 2001;21(10): 1133-1145.
6. Minoshima S, Giordani B, Berent S, Frey KA, Foster NL, Kuhl DE. Metabolic reduction in the posterior cingulate cortex in very early Alzheimer's disease. *Ann Neurol*. 1997;42(1):85-94.
7. Serrano-Pozo A, Frosch MP, Masliah E, Hyman BT. Neuropathological alterations in Alzheimer disease. 2011;1(1):a006189.
8. Jack CR, Knopman DS, Jagust WJ, et al. Hypothetical model of dynamic biomarkers of the Alzheimer's pathological cascade. *Lancet Neurol*. 2009;9(1):119-128.
9. Rojas S, Herance JR, Gispert JD, et al. In vivo evaluation of amyloid deposition and brain glucose metabolism of 5XFAD mice using positron emission tomography. *Neurobiology of Aging*. 2013;34(7):1790-1798.
10. Manook A, Yousefi BH, Willuweit A, et al. Small-Animal PET imaging of amyloid-beta plaques with [11C]PiB and its multimodal validation in an APP/PS1 mouse model of Alzheimer's Disease. *PLoS One*. 2012;7(3):e31310.
11. Maeda J, Ji B, Irie T, et al. Longitudinal, quantitative assessment of amyloid, neuroinflammation, and anti-amyloid treatment in a living mouse model of Alzheimer's Disease enabled by positron emission tomography. *J Neurosci*. 2007;27(41):10957-10968.
12. Sérrière S, Tauber C, Vercouillie J, et al. Neurobiology of Aging. *Neurobiol Aging*. 2015;36(4):1639-1614.
13. Luo F, Rustay NR, Ebert U, et al. Characterization of 7- and 19-month-old Tg2576 mice using multimodal in vivo imaging: limitations as a translatable model of Alzheimer's disease. *Neurobiology Aging*. 2012;33(5):933-944.
14. Poisnel G, Hérard AS, El Tannir N, et al. Increased regional cerebral glucose uptake in an APP/PS1 model of Alzheimer's disease. *Neurobiol Aging*. 2012;33(9):1995-2005.
15. Kuntner C, Kesner AL, Bauer M, et al. Limitations of small animal PET imaging with [18F]FDDNP and FDG for quantitative studies in a transgenic mouse model of Alzheimer's Disease. *Mol Imaging Biol*. 2009;11(4):236-240.

16. Rapic S, Backes H, Viel T, et al. Imaging microglial activation and glucose consumption in a mouse model of Alzheimer's disease. *Neurobiol Aging*. 2013;34(1):351-354.

17. Welch A, Mingarelli M, Riedel G, Platt B. Mapping changes in mouse brain metabolism with PET/CT. *J Nucl Med*. 2013;54(11): 1946-1953.

18. Macdonald IR, DeBay DR, Reid GA, et al. Early detection of cerebral glucose uptake changes in the 5XFAD mouse. *Curr Alzheimer Res*. 2014;11(5):450-460.

19. Martic-Kehl MI, Ametamey SM, Alf MF, Schubiger PA, Honer M. Impact of inherent variability and experimental parameters on the reliability of small animal PET data. *EJNMMI Res*. 2012; 2(1):26.

20. Wong KP, Sha W, Zhang X, Huang SC. Effects of administration route, dietary condition, and blood glucose level on kinetics and uptake of 18F-FDG in mice. *J Nucl Med*. 2011;52(5): 800-807.

21. Boellaard R. Standards for PET image acquisition and quantitative data analysis. *J Nucl Med*. 2009;50(suppl 1):11S-20S.

22. Abouzied MM, Crawford ES, Nabi HA. 18F-FDG Imaging: Pitfalls and Artifacts. *J Nucl Med Technol*. 2005;33(3):145-155.

23. Fueger BJ, Czernin J, Hildebrandt I, et al. Impact of animal handling on the results of 18F-FDG PET studies in mice. *J Nucl Med*. 2006;47(6):999-1006.

24. Deleye S, Verhaeghe J, Wyffels L, Dedeurwaerdere S, Stroobants S, Staelens S. Towards a reproducible protocol for repetitive and semi-quantitative rat brain imaging with 18 F-FDG: exemplified in a memantine pharmacological challenge. *Neuroimage*. 2014; 96:276-287.

25. Wahl RL, Henry CA, Ethier SP. Serum glucose: effects on tumor and normal tissue accumulation of 2-[F-18]-fluoro-2-deoxy-D-glucose in rodents with mammary carcinoma. *Radiology*. 1992; 183(3):643-647.

26. Toyama H, Ichise M, Liow JS, et al. Evaluation of anesthesia effects on [18F]FDG uptake in mouse brain and heart using small animal PET. *Nucl Med Biol*. 2004;31(2):251-256.

27. Saha JK, Xia J, Grondin JM, Engle SK, Jakubowski JA. Acute hyperglycemia induced by ketamine/xylazine anesthesia in rats: mechanisms and implications for preclinical models. *Exp Biol Med*. 2005;230(10):777-784.

28. Flores JE, McFarland LM, Vanderbilt A, Ogasawara AK, Williams SP. The effects of anesthetic agent and carrier gas on blood glucose and tissue uptake in mice undergoing dynamic FDG-PET imaging: sevoflurane and isoflurane compared in air and in oxygen. *Mol Imaging Biol*. 2008;10(4):192-200.

29. Matsumura A. Assessment of microPET performance in analyzing the rat brain under different types of anesthesia: comparison between quantitative data obtained with microPET and ex vivo autoradiography. *Neuroimage*. 2003;20(4):2040-2050.

30. Vachon P, Moreau JP. Serum corticosterone and blood glucose in rats after two jugular vein blood sampling methods: comparison of the stress response. 2001;40(5):22-24.

31. De Boer SF, Koopmans SJ, Slangen JL, Van Der Gugten J. Plasma catecholamine, corticosterone and glucose responses to repeated stress in rats: effect of interstressor interval length. *Physiol Behav*. 1990;47(6):1117-1124.

32. Meijer MK, Lemmens AG, Van Zutphen BF, Baumans V. Urinary corticosterone levels in mice in response to intraperitoneal injections with saline. *J Appl Anim Welf Sci*. 2005;8(4): 279-283.

33. Howlett DR, Bowler K, Soden P, Riddell DR, Davis JB. Aβ Deposition and Related Pathology in an App X Ps1 Transgenic Mouse Model of Alzheimer's Disease. *Histol Histopathol*. 2008; 23(1):67-76.

34. Kelley J, Wintmolders C, Bottelbergs A, et al. Investigations of brain glucose utilization in three transgenic mouse strains that develop neuropathological features of Alzheimer's disease. *Alzheimers Dement*. 2013;9(4): P329.

35. Waldron AM, Wyffels L, Verhaeghe J, et al. Quantitative μPET imaging of cerebral glucose metabolism and amyloidosis in the TASTPM double transgenic mouse model of Alzheimer's disease. *Curr Alzheimer Res*. 2015;12(7):694-703.

36. Waldron AM, Wyffels L, Richardson J, et al. Longitudinal monitoring of β-amyloid pathology and cerebral hypometabolism in a double transgenic mouse model of Alzheimer's disease. *Alzheimers Dement*. 2014;10(4): P27.

37. Howlett DR, Richardson JC, Austin A, et al. Cognitive correlates of Aβ deposition in male and female mice bearing amyloid precursor protein and presenilin-1 mutant transgenes. *Brain Res*. 2004;1017(1):130-136.

38. Kemp BJ, Hruska CB, McFarland AR, Lenox MW, Lowe VJ. NEMA NU 2-2007 performance measurements of the Siemens Inveon preclinical small animal PET system. *Phys Med Biol*. 2009;54(8):2359-2376.

39. Hudson HM, Larkin RS. Accelerated image reconstruction using ordered subsets of projection data. *IEEE Trans Med Imaging*. 1994;13(4):601-609.

40. Defrise M, Kinahan PE, Townsend DW, Michel C, Sibomana M, Newport DF. Exact and approximate rebinning algorithms for 3-D PET data. *IEEE Trans Med Imaging*. 1997;16(2):145-158.

41. Watson CC. New, faster, image-based scatter correction for 3D PET. *IEEE T Nucl Sci*. 2000;47(4):1587-1594.

42. Schiffer WK, Mirrione MM, Biegon A, Alexoff DL, Patel V, Dewey SL. Serial microPET measures of the metabolic reaction to a microdialysis probe implant. *J Neurosci Meth*. 2006;155(2): 272-284.

43. Mirrione MM, Schiffer WK, Fowler JS, Alexoff DL, Dewey SL, Tsirka SE. A novel approach for imaging brain–behavior relationships in mice reveals unexpected metabolic patterns during seizures in the absence of tissue plasminogen activator. *Neuroimage*. 2007;38(1):34-42.

44. Deleye S, Verhaeghe J, Wyffels L, Dedeurwaerdere S, Stroobants S, Staelens S. Towards a reproducible protocol for repetitive and semi-quantitative rat brain imaging with 18 F-FDG: exemplified in a memantine pharmacological challenge. *Neuroimage*. 2014; 96:276-287.

45. Mosconi L.Brain glucose metabolism in the early and specific diagnosis of Alzheimer's disease. FDG-PET studies in MCI and AD. *Eur J Nucl Med Mol I*. 2005;32(4):486-510.

46. Klunk WE, Engler H, Nordberg A, et al. Imaging brain amyloid in Alzheimer's disease with Pittsburgh Compound-B. *Ann Neurol*. 2004;55(3):306-319.

47. Small GW, Kepe V, Ercoli LM, et al. PET of brain amyloid and tau in mild cognitive impairment. *N Engl J Med*. 2006;355(25): 2652-2663.

48. Rapic S, Backes H, Viel T, et al. Imaging microglial activation and glucose consumption in a mouse model of Alzheimer's disease. *Neurobiol Aging*. 2013;34(1):351-354.

49. Nowland MH, Hugunin KMS, Rogers KL. Effects of short-term fasting in male Sprague-Dawley rats. *Comp Med*. 2011;61(2): 138-144.

50. Jensen T, Kiersgaard M, Sorensen D, Mikkelsen L. Fasting of mice: a review. *Lab Animals*. 2013;47(4):225-240.

51. Sugawara Y, Zasadny KR, Neuhoff AW, Wahl RL. Reevaluation of the standardized uptake value for FDG: variations with body weight and methods for correction. *Radiology*. 1999;213(2): 521-525.

52. Kim CK, Gupta NC, Chandramouli B, Alavi A. Standardized uptake values of FDG: body surface area correction is preferable to body weight correction. *J Nucl Med*. 1994; 35(1):164-167.

53. Thie JA, Hubner KF, Isidoro FP, Smith GT. A weight index for the standardized uptake value in 2-deoxy-2-[F-18]fluoro-d-glucose-positron emission tomography. *Mol Imaging Biol*. 2007;9(2):91-98.

54. Toyama H, Ye D, Ichise M, et al. PET imaging of brain with the β-amyloid probe, [11C]6-OH-BTA-1, in a transgenic mouse model of Alzheimer's disease. *Eur J Nucl Med Mol I*. 2005; 32(5):593-600.

55. Flood DG, Lin YG, Lang DM, et al. A transgenic rat model of Alzheimer's disease with extracellular Abeta deposition. *Neurobiol Aging*. 2009;30(7):1078-1090.

56. Teng E, Kepe V, Frautschy SA, et al. [F-18]FDDNP microPET imaging correlates with brain Aβ burden in a transgenic rat model of Alzheimer disease: effects of aging, in vivo blockade, and anti-Aβ antibody treatment. *Neurobiol Dis*. 2011;43(3):565-575.